AMERICAN JOURNAL OF BIOSCIENCE AND CLINICAL INTEGRITY
https://biojournals.us/index.php/AJBCI
ISSN: 2997-7347

Article

Effects of Low-Energy Ion Implantation on the Physicochemical Properties of Si Oxides

Allayarova Gulmira Xolmuratovna[1], Allanazarova Sarvinoz Shavkat qizi[2]

1. Associate Professor, PhD Department of Theoretical and Experimental Physics, Faculty of Physics, Karshi State University, Karshi, 180117 Uzbekiston
2. Master's student Department of Theoretical and Experimental Physics, Faculty of Physics, Karshi State University, Karshi, 180117 Uzbekiston
*Correspondence: allayarova5030@mail.ru

Citation: Xolmuratovna A. G., Shavkat qizi A. S. Effects of Low-Energy Ion Implantation on the Physicochemical Properties of Si Oxides. American Journal Of Bioscience And Clinical Integrity 2026, 3(2), 128-133.

Received: 10th Nov 2025
Revised: 11th Dec 2025
Accepted: 23th Jan 2026
Published: 24th Feb 2026

Abstract: Thin SiO2 films were obtained by implanting O2+ ions into Si combined with thermal annealing. Oxide films obtained in an UHV setup by thermal oxidation were also used for comparison. Auger electron spectra revealed that these regions contain Si atoms (Figure 2). The degree of coverage of the Si surface with silicon oxide was estimated by the ratio of the area of the Auger peak L23VV of silicon in Si (91 eV) and in SiO2 (76 eV). By varying the ion dose within the range from ~ 8•1015 to 4•1016, the sizes of nanosites can be regulated within the range from 5 – 10 nm to 20 – 25. At D ≤ 8•1016 cm-2, the formation of an island film of SiO2 was observed. Based on experimental studies, it was established that when bombarding SiO2 with Ar+ ions in the surface region of SiO2 at low doses (D ≤5• 1015 cm-2), individual nanocluster regions enriched with up to 50–60 at.%.

Keywords: Nanoscale structures, heterostructures, high-frequency, crystalline structure, emission and optical properties.

Introduction

Nanoscale structures and multilayer systems based on Si and SiO_2 hold promise for the creation of nano- and optoelectronic devices. In particular, SiO_2/Si heterostructures with various nanoinclusions serve as the basis for the development of new types of high-frequency MOS transistors, integrated circuits, optical converters, and solar cells. In this regard, obtaining structurally perfect nanoscale films of molybdenum and silicon oxides, studying their electronic and crystalline structure, emission and optical properties and modifying these properties by ion bombardment is a pressing task of modern physical electronics[1-6].

In this regard, special attention is being paid to improving the technology for producing and studying the formation patterns of nanoscale structures with new physical properties. The creation of nanoscale multilayer structures with tailored physical properties is of greatest scientific

and applied significance[7-9]. However, issues related to producing continuous, homogeneous films with a thickness of less than 50-60 Å on the surface of various materials remain unresolved.

Methods

To accomplish the tasks set in the work, it was necessary to carry out technological processing of samples (thermal annealing, ion implantation, film deposition on the surface, laser annealing) in the same experimental device and under identical conditions, as well as to study their physicochemical properties using a set of methods of secondary electron spectroscopy (SES) and photoelectron spectroscopy (PES). Individual experiments were conducted in an LAS-2200 ultrahigh vacuum (UHV) setup. The objects of study were single-crystal Si(111) samples, amorphous films, and single-crystal SiO_2 (α-quartz) samples. Thin SiO_2 films were obtained by implanting O_2^+ ions into Si combined with thermal annealing. Oxide films obtained in an UHV setup by thermal oxidation were also used for comparison. Si preparation was performed as follows: after polishing, the samples were rinsed in acetone, boiled in a mixture of hydrogen peroxide (~6%) and HSE (48%) solutions for 5 minutes, then a portion of the silicon oxide was removed from the surface in a hydrofluoric acid solution, and then the samples were rinsed several times in distilled water. After drying, the samples were installed in the UHV device.

Results and discussions

In the case of Si(111) samples, their degassing was carried out at T≈ 1200 K for 4-5 hours and at T=1500 K for a short time in combination with gentle etching of the surface with Ar^+ ions. Amorphous films and single-crystal SiO_2 samples were degassed at T≈ 900 K for 2-3 hours in a vacuum of no worse than 10^{-7} Pa.

As an example, Fig. 1 shows an SEM image of the surface of a SiO_2 film obtained after heating at T = 1100 K of silicon implanted with O_2^+ ions with an energy of E_0 = 3 keV at D = 10^{16} cm^{-2}.

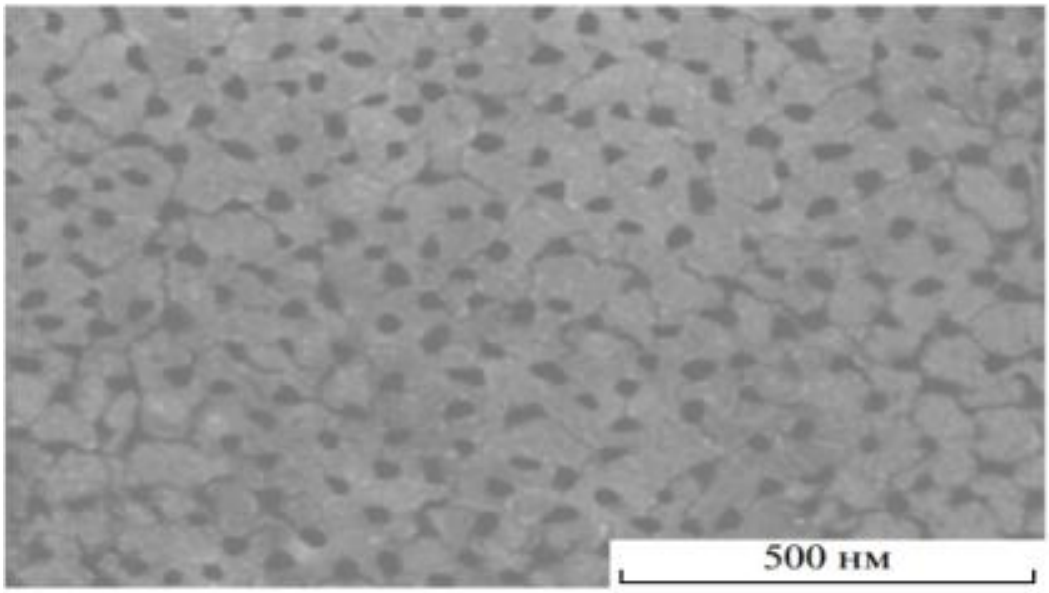

Figure 1. SEM images of the SiO_2/Si(111) surface with nanocrystalline phases of Si atoms

Figure 1 shows that clearly defined regions are forming between the crystalline phases, and the boundaries of individual crystalline phases are beginning to emerge. Analysis of the Auger electron spectra revealed that these regions contain Si atoms (Figure 2). The degree of coverage of the Si surface with silicon oxide was estimated by the ratio of the area of the Auger peak $L_{23}VV$ of silicon in Si (91 eV) and in SiO_2 (76 eV):

$$\theta = \frac{I_{Si}(91\ эВ)}{I_{SiO_2}(76\ эВ)} = \frac{\Delta S_{Si}(91\ эВ)}{\Delta S_{SiO_2}(76\ эВ)} \quad (1)$$

This ratio for this case was 0.90 – 0.92. Moreover, if we take into account that the distance between the centers of neighboring clusters is within 50 – 60 nm [69], then the density of nanosites that are sinks for Si is 10^{10}–10^{11} cm^{-2}.

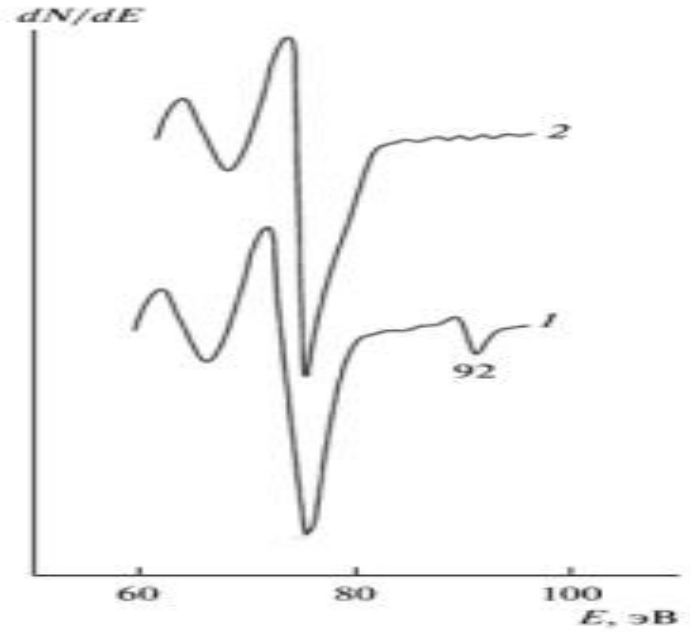

Figure 2. The initial part of the Auger spectrum of SiO_2 films obtained after annealing Si implanted with ions with energy E_0 = 3 keV at doses D, cm^2; 1– 10^{16}; 2– 8 10^{16} cm^{-2}.

The average diameter of each individual nanosite is ~ 12 – 15 nm. By varying the ion dose within the range from ~ 8•10^{15} to 4•1016, the sizes of nanosites can be regulated within the range from 5 – 10 nm to 20 – 25. At D ≤ 8•10^{16} cm^{-2}, the formation of an island film of SiO_2 was observed.

Based on experimental studies, it was established that when bombarding SiO_2 with Ar^+ ions in the surface region of SiO_2 at low doses (D ≤5• 10^{15} cm^{-2}), individual nanocluster regions enriched with up to 50−60 at.% Si atoms are formed, and at high doses (D ≥ 6•10^{16} cm^{-2} 10^{16} cm^2), a thin layer (d = 2.5−3.0 nm) of pure silicon in the form of individual blocks is formed (Fig. 3). After heating, the film decomposes into individual cluster phases of pure Si. At T = 700 K, the surface dimensions of these phases are ~200-400 nm, and the distance between them is ~300-500 nm. The thickness of the cluster phases increases to 3.0-4.0 nm. Increasing T to 900 K leads to evaporation of the silicon phases.

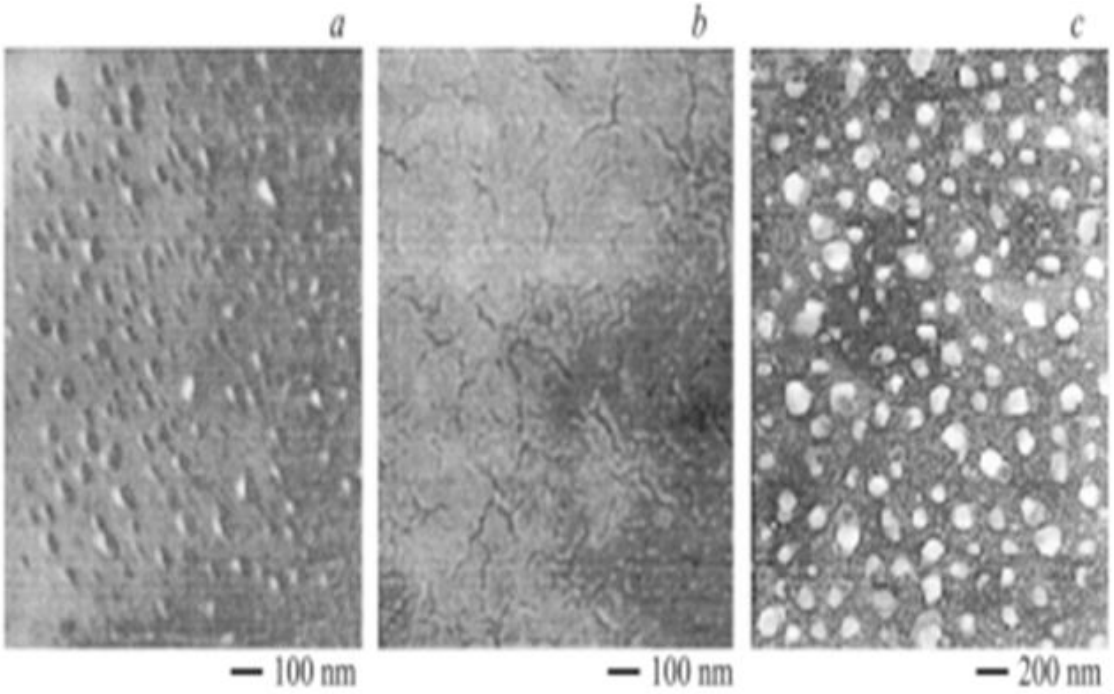

Figure 3. SEM images of the SiO_2 surface irradiated with Ar^+ ions with E_0 = 1 keV at doses D, cm^2, a – 10^{15} b - $6 \cdot 10^{16}$, c - $6 \cdot 10^{16}$, after heating the samples at T=700K.

In [5-12] it is shown that when bombarding SiO_2 films with Ba^+ ions at a high dose, the value of e^{φ} surface σ_m — decreases to 2.3 eV, and the value increases to 3.8. In this case, the surface is covered with a monolayer of BaO with some excess of Ba, and in the near-surface layer a compound of the type BaO, Ba – Si – O, Ba – Si with a thickness of 50–60 Å is formed. In the case of ion-implanted SiO_2 films, the $Ba_{0.4}Si_{0.6}O_2$ type compound exhibits the highest emission efficiency.

To evaluate the emission efficiency of the constituent ion-implanted layers, the authors of the work [6-20] created BaO, $BaSi_2$, and $Ba_{0.4}Si_{0.6}O_2$ films by sputtering them onto the SiO_2 surface and investigated their emission properties. These results are presented in Table 1, which are compared with the data obtained for a SiO_2 film implanted with Ba^+ ions with E_0=1 keV at D = 6 $\cdot 10^{16}$ cm^{-2}.

Table 1. Composition and emission properties of the studied films.

Objects of research	Film composition	Film thickness, Å	eφ	E_g	σ_m	λ /Å
SiO_2/Si	SiO_2	1000	4,7	8,9	2,8	300-350 500-550
$Ba^+ \rightarrow\rightarrow$ SiO_2(E_0 =1 кэВD = 6 10^{16} cm^{-2})	BaO, Ba- Si-O Ba- Si, Ba, Si,	50-60	2,3	5,3	3,8	
BaO/SiO_2	BaO	300	2,6	3,9	2,3	-
$Ba_{0,4}Si_{0,6}O_2/SiO_2$	$Ba_{0,4}Si_{0,6}O_2$	300	4,6	6,6	3,2	-
SiO_2 c monolayer film BaO+Ba			2,3	8,9	4,8	-

Eg^*- average values E_g.

From Table 1 it can be seen that the band gap width Eg and, consequently, the emission efficiency of the $Ba_{0,4}Si_{0,6}O_2$ film is significantly greater than Eg for BaO and $BaSi_2$, but less than Eg for the undoped SiO_2 film. Despite this, the zone of exit λ of truly secondary electrons after ion implantation increases by 1.5 times or more and is 500-550 Å, which significantly exceeds the thickness of the ion-doped layer, even taking into account the diffusion of implanted Ba atoms into the depth of the sample, caused by the concentration gradientIt should be noted that for the same values of eφ, the values of ion-doped Si are noticeably (~ 1.2-2 times) greater than for SiO_2 in the presence of a monolayer BaO+Ba film.

Conclusion

In the case of ion-implanted SiO_2 films, the $Ba_{0.4}Si0.6O_2$ type compound exhibits the highest emission efficiency. To evaluate the emission efficiency of the constituent ion-implanted layers, the authors of the work created BaO, $BaSi_2$, and $Ba_{0.4}Si0.6O_2$ films by sputtering them onto the SiO_2 surface and investigated their emission properties. Determination of the size, chemical state and their influence on the electronic structure (in particular, the band gap) of nanostructures at localized different depths of the SiO2 film under ion bombardment.

REFERENCES

[1] High Temperature Structural Silicides// Proc.of the First High Temperature Structural Silicides Workshop, USA, 1991 – Elsevier Sci.Publ., Amsterdam, 1992. P.278.

[2] Е. П., Нечипоренко, А.П., Петриченко Ю.Б., Павленко// Защита металлов от коррозии.- Харьков: Вища школа,1985.- 112С

[3] С.В. Литовченко , В.М. Береснев, А.А. Дробышевская, П.В. Турбин // Силицидные покрытия на молибдене: получение структура, свойства / Физическая инженерия поверхности. 2012. Т.10, №2. С.110–137. Бібліогр.: 65 назв. — рос. http://dspace.nbuv.gov.ua/handle/123456789/98941

[4] Ю.А. Петухов., Н.Т. Квасов., В.В. Углов., В.М. Асташинский А. М. Кузьмицкий // Структура и фазовый состав системы молибден- кремний, обработанной компрессионными плазменными потоками / Доклады Белорусского государственного университета информатики и радиоэлектроники 2011 № 1 (55) С. 31-37

[5] https://cyberleninka.ru/article/n/struktura-i-fazovyy-sostav-sistemy-molibden-kremniy-obrabotannoy-kompressionnymi-plazmennymi-potokam

[6] Ivanenko L.I., Shaposhnikov V.L., Filonov A.B., et al. // Thin solid films. 2004. Vol. 461. P. 141-147.

[7] Galkin N.G., Chusovitin E.A., Goroshko D.L. et al. // Journal of Physics D: Applied Physics. 2007. Vol. 40, №17. P. 5319.

[8] Esconjauregui S., Whelan C.M., Maex K. // Nanotechnology. 2007. Vol. 18. P. 015602.

[9] Iriarte G.F. // Journal of Non-Crystalline Solids. 2010. Vol. 356. P. 1135-1144.

[10] Legagneux P., Pribat D, Nedellec Y. // US Patent 7491269. 2009. Chen L.J. // JOM. 2004. Vol. 57, № 9. P. 24-31.

[11] Qiuyu Chena , Shuhua Lianga,, Bingxue Lia , Zheng Chena,, Xiaoyan Songc, Longchao Zhuoa// Versionof Record: 2021 published by Elsevier. This manuscript is made available under the Elsevier user license https://www.elsevier.com/open-access/userlicense/1.0/

[12] Kong Yakang , Cheng Wang , Xiancong Chen, Yi Qu , Jiabo Yu, Haijuan Ju and Xiao Yilei // Submission received: 6 July 2023 / Revised: 25 July 2023 / Accepted: 26 July 2023 / Published: 7 August 2023 https://doi.org/10.3390/ma16155495

[13] Mi Zhao, Wei Ye, Mengyuan Zhu, Yuteng Gui, Wei Guo, Shusen Wu 2 and Youwei Yan// Submission received: 7 October 2022 / Revised: 4 November 2022 / Accepted: 11 December 2022 / Published: 20 December 2022 https://doi.org/10.3390/ma16010003

[14] Lu Wang, Meng-Chao Li, Guo-Hua Zhang, and Zheng-Liang Xue// Published by De Gruyter November 30, 2020 https://doi.org/10.1515/htmp-2020-0093

[15] Nikolai V. Alov// physica status solidi 09 February 2015 - Wiley Online Library **https://doi.org/10.1002/pssc.201400108**

[16] Allayarova, G. Kh.// Journal of Surface Invesgation. 2020 Vol.14., Issue.6.,Page.,1179-1182. DOI:10.1134/S1027451020060026

[17] Isakhanov Z. A., Mukhtarov Z. E., Umirzakov B. E., Ruzibaeva M. K. // Technical physics. V. 56, № 4, P.546-549. DOI: 10.1134/S1063784211040177. 2011,

[18] Donaev S. B., Tashatov A. K., Umirzakov B. E. 2015, V.9, №2, P.406-409. DOI: 10.1134/S1027451015020263.

[19] Umirzakov B.E., Imanova G.T., Bekpulatov I.R., Turapov I.K. Obtaining of thin films of manganese silicides on a Si surface by the method of solid-phase deposition and investigation of their electronic structure. Modern Physics Letters., 2023, 37(24), 2350078.

[20] Allayarova G.Kh. Tashmukhamedova, DA; Yusupjanova, MB; Umirzakov, BE // Technical physics. 2020., V.46. Issue.10. P.972-975. DOI:10.1134/S1063785020100144.

[21] Elmurotova D.B., Kattaxodjayeva D.U., Tanirbergenova N.O. The Main Tasks of Biophysics and the Physical Foundations of Biological Structures// American Journal of Bioscience and Clinical Integrity, ISSN: 2997-7347, V.2, N.10, 2025, October P.71-77. https:///biojournals.us/index.php/AJBCI/article/view/1596/1345

[22] Elmurotova D.B., Imamova L.N., Orifqulova M.F. Indications for holter monitoring // Miasto Prysztosci, IF-9.9, ISSN-L:2544-980X, V.62, 2025, P.155-160. Poland. https://miastoprzyszlosci.com.pl/index.php/mp/article/view/6828

[23] Elmurotova D.B., Qo'ziyev S.R. Retinitis pigmentosa: clinical picture and diagnostic insights // Western European Journal of Linguistics and Education, ISSN (E): 2942-190X, V.3, Issue 10, October 2025, P.113-120. Germany, https://westerneuropeanstudies.com/index.php/2/article/view/2901/20091

[24] Elmurotova D.B., Qo'ziyev S.R. Current Perspectives on the Etiology and Epidemiology of Retinitis Pigmentosa // American Journal of Bioscience and Clinical Integrity, ISSN: 2997-7347, V.2, N.10, 2025, October P.119-124. America. https://biojournals.us/index.php/AJBCI/article/view/1641/1380

[25] Elmurotova D.B., Urmanbekova D.S., Bozorov M.B. Main risk factors of myocardial infarction // American Journal of Bioscience and Clinical Integrity, ISSN: 2997-7347, V.2, N.12, 2025, Dekabr P.6-9. https://biojournals.us/index.php/AJBCI/article/view/1763/1476